

PROCEEDINGS OF SPIE

SPIDigitalLibrary.org/conference-proceedings-of-spie

Optical design of the wavefront sensing in the ULTIMATE-Subaru Ground Layer Adaptive Optics system

Yoko Tanaka, Yosuke Minowa, Yoshito Ono, Koki Terao, Hiroshige Yoshida, et al.

Yoko Tanaka, Yosuke Minowa, Yoshito Ono, Koki Terao, Hiroshige Yoshida, Masayuki Akiyama, Noelia Martínez Rey, Nicholas Herral, Céline d'Orgeville, François Rigaut, Israel Vaughn, David Chandler, Dionne Haynes, Warrick Schofield, "Optical design of the wavefront sensing in the ULTIMATE-Subaru Ground Layer Adaptive Optics system," Proc. SPIE 12185, Adaptive Optics Systems VIII, 121856M (29 August 2022); doi: 10.1117/12.2629581

SPIE.

Event: SPIE Astronomical Telescopes + Instrumentation, 2022, Montréal, Québec, Canada

Optical design of the Wavefront sensing in the ULTIMATE-Subaru Ground Layer Adaptive Optics system

Yoko Tanaka^a, Yosuke Minowa^a, Yoshito Ono^a, Koki Terao^a, Hiroshige Yoshida^a, Masayuki Akiyama^b, Noelia Martinez Rey^c, Nicholas Herral^c, Celine D'Orgeville^c, Francois Rigaut^c, Israel Vaughn^c, David Chandler^c, Dionne Haynes^c, and Warrick Schofield^c

^aSubaru Telescope, 650 N.Aohoku Place, Hilo, HI, 96720 U.S.A.

^bTohoku University, 6-3, Aramaki Aza-Aoba, Aoba-ku, Sendai 980-8578, Japan

^cAustralian National University, Canberra ACT 2601, Australia

ABSTRACT

ULTIMATE-Subaru (Ultra-wide Laser Tomographic Imager and MOS with AO Transcendent Exploration) is the next-generation development project of the Subaru Telescope in Hawaii, U.S.A. Ground Layer Adaptive Optics (GLAO) technology corrects atmospheric turbulence near the ground and improves the star image to realize wider fields of view (14 x 14 arcmin) than conventional adaptive optics can do. In the GLAO system, the laser launch system emits four lasers of up to 20 minutes of asterism, then these four lasers excite four artificial stars from 80km to 200km in the sky. The wavefront sensor (WFS) system observes them and corrects atmospheric turbulence. The WFS system also utilizes four natural stars outside the science field of view as well. This paper presents the preliminary optical design of the WFS system.

Keywords: GLAO, Wavefront sensor, optical design

1. INTRODUCTION

ULTIMATE-Subaru implements the Ground Layer Adaptive Optics (GLAO) system, which has a wide field coverage of as much as 14x14 square minutes. The GLAO system consists of an adaptive secondary mirror (ASM), four laser guide stars (LGSs) to generate an asterism up to 20 arcmin in diameter, four LGS wavefront sensors (WFSs) focusing on the finite distance from 80km to 200km, and natural guide star (NGS) WFSs for low-order tip/tilt and focus correction. The WFS for LGS consists of a pick-off mirror, collimator, telescope aberration (Astigmatism) compensator, microlens array (MLA), and relay optics. The WFS for NGS consists of a pick-off mirror, collimator, and 2x2 lens array (or camera lens). To compensate for the telescope's non-telecentricity, the pick-off mirrors must be controlled concerning the field angle. Since Subaru Telescope is a Ritchey-Chretien type telescope, astigmatism aberration is dominant at Cassegrain (Cs.) focus. To compensate for this astigmatism, we placed two optical elements with a Zernike surface near the pupil position. The WFS is installed in the space above the wide-field imaging device, as shown in Fig. 1. The yellow and blue colored areas in Fig.1 show the space for the LGS and the NGS WFS, respectively. All the optical and opto-mechanical components must fit in this space.

2. SPECIFICATIONS

Tab.2 shows the specifications required to the WFS system. The area of NGS is outside of the science field of view as shown in Fig.2. We assume that sCMOS cameras (ORCA-Fusion BT from Hamamatsu Photonics) are used for both of the LGS and the NGS WFS systems.

From the NGS pixel scale, in single-eye mode, the camera's F-number is 0.56, making aberration correction almost impossible. When binning processing is adopted, the focal lengths and F-numbers are listed in Tab.2. Even in 2x2 binning mode, the F-number is about 1, and still, it is hard to correct aberration. Therefore we adopted 4x4 binning mode for the NGS system camera as shown in Tab.2. In addition, it had been confirmed by other simulations that the performance of GLAO is not affected even in the 4x4 binning mode.

Further author information: Yoko Tanaka: E-mail: yoko@naoj.org

Adaptive Optics Systems VIII, edited by Laura Schreiber, Dirk Schmidt, Elise Vernet,
Proc. of SPIE Vol. 12185, 121856M · © 2022 SPIE
0277-786X · doi: 10.1117/12.2629581

Proc. of SPIE Vol. 12185 121856M-1

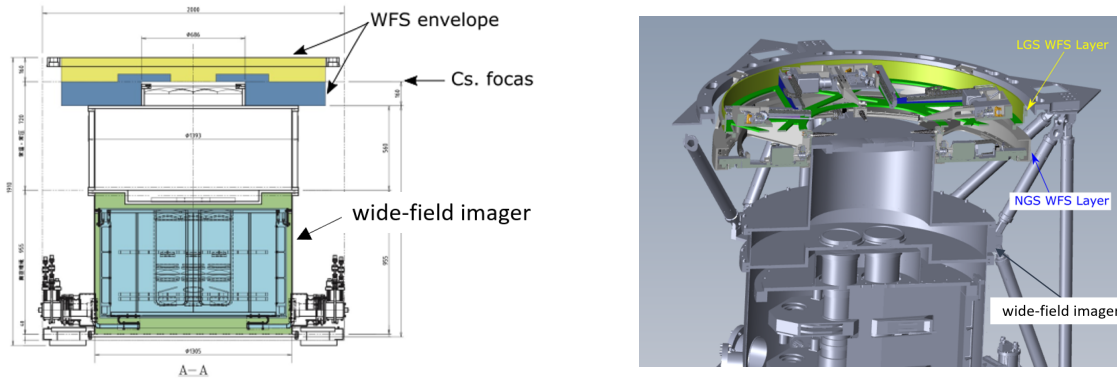


Figure 1. Envelope drawing (left) and 3D instrument model (right). The yellow area of the left figure shows the space for the LGS system and the blue area shows the space for the NGS system.

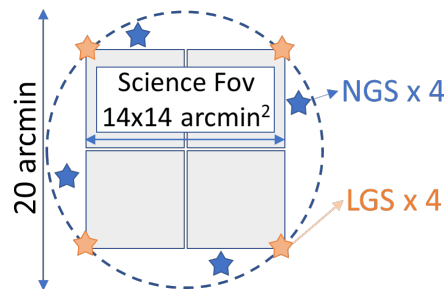


Figure 2. The diagram of patrol area of LGS and NGS

3. LAYOUT DESIGN

Since the Subaru Telescope is a Ritchey-Chrétien type at the Cs focus, there is a remaining astigmatism aberration at the focal plane and it increases toward the edge of the field. In addition, as the field of view increases, the position of the best focus moves away from the nominal focal plane at the field center due to the field curvature shown in Fig.3. In Fig.3, the Y-axis represents the best focus position from the pick-off mirror, and + indicates that the best focus is in front of the pick-off mirror. Considering the size of the mirror, etc., in the field of view of 9 minutes or above in NGS, the best focus comes in front of the pick-off mirror, which makes it difficult to install a field stop.

To keep the focus within the NGS WFS optical path to have a field stop, we considered three layouts as shown in Fig.4. Ver.1 is the original configuration that does not allow us to install the field stop for the NGS WFS at the edge of the field of view. In Ver.2 and Ver.3, the NGS WFS (and the LGS WFS as well in the case of Ver.3) moves along the inclined surface that best fits the curved focal plane. The angle of the inclination is about 3.4 degrees. In this case, the NGS field stop can be installed within the optical path. Considering the space allocated to the WFS system, we decided to proceed with the design of Ver.3. The focus adjustment for each field of view is performed by moving the unit of the entire optical system after the field stop. We change the distance between the pick-off mirror to the field stop for focusing to the best position for each field of view. The Ver.3 layout can also minimize the range of the focus adjustment both for the NGS and the LGS WFSs.

3.1 Pick-off mirror

The light from the telescope is introduced into WFS system by the pick-off mirror, and the pupil image is created by the collimator lens. In the case of the LGS WFS, the pupil is divided into 32x32 by a Micro-Lens Array

Table 1. Specifications of the GLAO WFS system

	NGS	LGS
sensor number	4	4
patrol area(radius)	7~10[arcmin]	2~10[arcmin]
star height	infinity	80~200[km]
field of view	ϕ 5[arcsec]	ϕ 7[arcsec]
pupil division number	single (for three sensors) and 2x2	32 x 32
pixel scale	0.3[arcsec/pixel] ¹	1.0[arcsec/pixel]
pixel size	26[um] (4x4 binning) ²	6.5[um]
wavelength	550~900[nm]	589[nm]
spot RMS radius	<0.15[arcsec]	<0.64[arcsec]

¹ 4x4 binning mode² physical pixel size is 6.5[um]

Table 2. F-number of NGS Camera

	no binning	2x2 binning	4x4 binning
camera focal length	6.7[mm]	13.4[mm]	26.7[mm]
F#	0.54	1.09	2.17

(MLA), and each Shack-Hartmann spot is re-imaged on the detector through a relay lens. In the case of the NGS WFS, one of the four WFSs is divided into 2x2, and the other three are not divided (single-eye mode). Tip/Tilt measurement is performed by the four NGS WFSs, and focus change due to the height of LGS is measured with the single 2x2 NGS WFS. For NGS WFSs, lights from the telescope are picked up at the position shown by the red dotted line in Fig.3. For LGS WFS, the pick-off mirror moves along the inclined surface that is the same with the NGS WFS, picking up light from the telescope, but located 70mm above the slope of NGS WFS. Since the Subaru Telescope is not telecentric, the angle of the chief ray differs from each field of view. Therefore, to prevent the pupil image at the lens array position from shifting, the angle of the pick-off mirror should be controlled according to the chief ray angle as shown in Fig.5. Actual numbers of pick-off mirror angles are also shown in Fig.5.

3.2 Astigmatism compensator

As described above, the remaining astigmatism at the Cs focus is large at the field edge where the LGSs and NGSs are located. To remove this static aberration due to the telescope optics, we introduced astigmatism correction plates that can adjust the correction amount depending on the location in the field of view. The principle can be found in the reference.¹ In the WFS optical path, we simply put a pair of parallel plates with the same Zernike surface but reversed signs, and rotate each plate in opposite directions by the same angle.

At first ($\beta = 0$), they canceled each other and astigmatism is zero. It can be seen that the astigmatism increases as the rotation angle increases as shown in Fig.6. From the equation1, this has the maximum correction amount at $\beta = 45$ degrees.

Table 3. Optical numbers of WFS

NGS	
Collimator focal length	150[mm]
Pupil size	$\phi 12.2$ [mm]
Camera focal length	26.7[mm] (4x4 binning mode)
LGS	
collimator focal length	116.6[mm]
Pupil size	$\phi 9.55$ [mm]
MLA focal length	8.725[mm]
magnification of relay	0.18

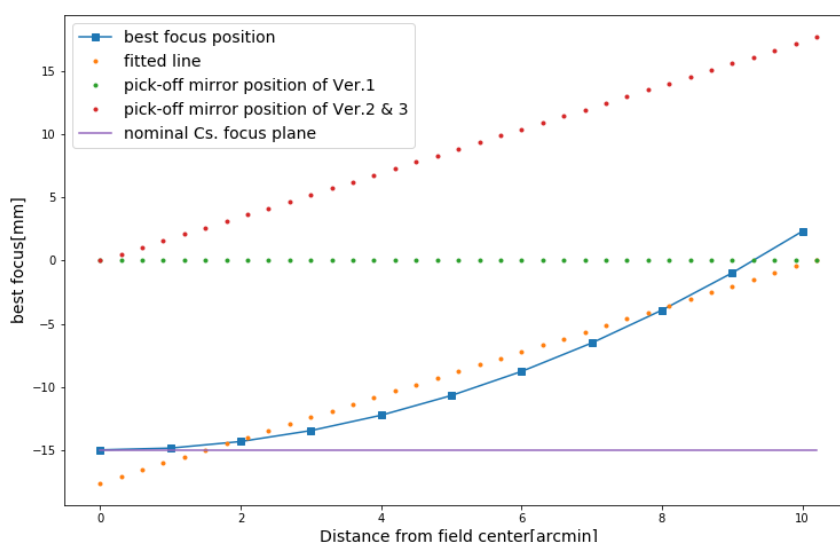


Figure 3. The best focus plot of NGS with respect to telescope field. The orange dotted line shows the best fitted line to the best focus curve. The green dotted line shows the pick-off mirror position of Ver.1 in Fig.4. The red dotted line, which is parallel to the orange line, shows the pick-off mirror position of Ver.2 and 3 in Fig.4. The actual best fitted line is slightly different from this line because WFS system uses fields from 2 arcmin to 10 arcmin.

$$\text{Zernike 5th term} = \rho^2(\sin 2\phi)$$

$$\begin{aligned} S1 + S2 &= a(\rho^2(\sin 2(\phi + \beta))) - a(\rho^2(\sin 2(\phi - \beta))) \\ &= 2a \sin 2\beta \cdot \rho^2 \cos 2\phi \\ &= 2a \sin 2\beta \cdot (\text{Zernike 6th term}) \end{aligned} \quad (1)$$

The magnitude of the Zernike term is such that the astigmatism component in the patrol field of view of 10 minutes can be corrected at 45 degrees. Figure7 is a wavefront aberration map before and after the astigmatism correction. We can see that astigmatism caused by the telescope is corrected in the entire patrol field of view by changing the rotation angle of the astigmatism correction plate.

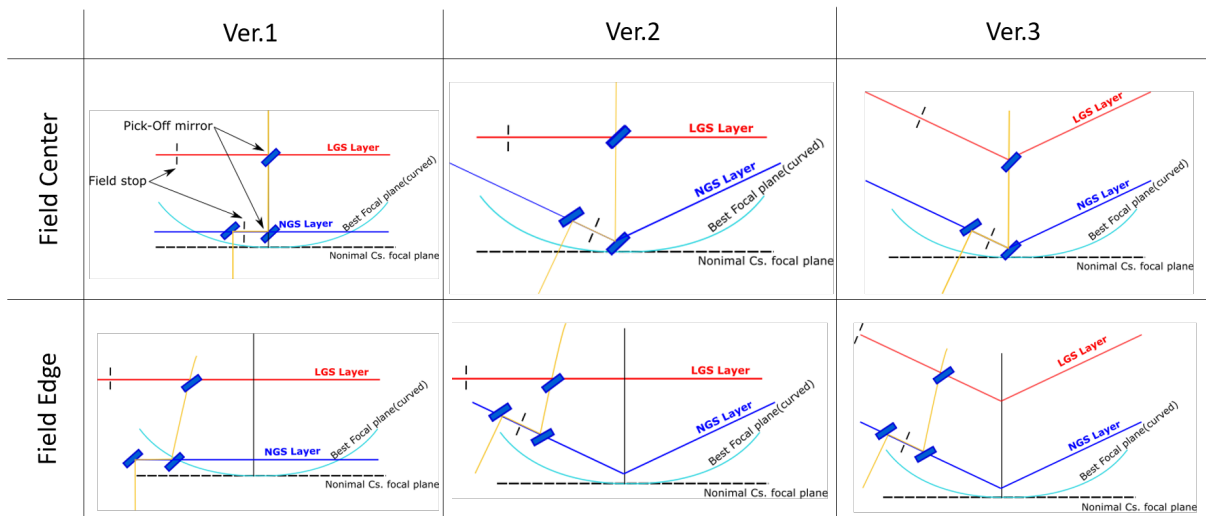


Figure 4. Three layout ideas. At the field edge of ver.1, we cannot install a field stop because the best focus position is the front of the pick-off mirror.

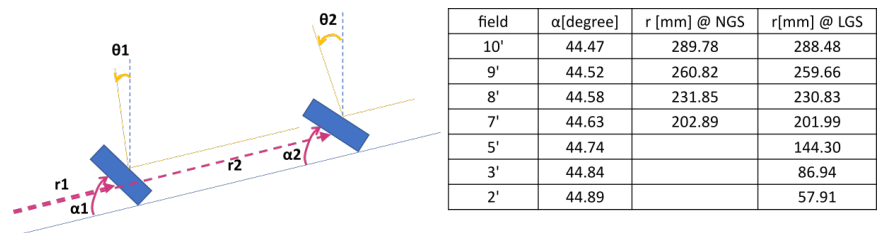


Figure 5. A schematic diagram of the adjustable pick-off mirror

4. OPTICAL DESIGN

4.1 NGS WFS

Fig.8 shows the layout of the collimator for the NGS WFS. Chromatic aberration correction is essential because the NGS WFS covers a broad wavelength range. Therefore, we adopted a doublet lens as a collimator. Fig.9 shows the layout of the camera lens for the NGS WFS single-eye mode. This camera lens consists of a doublet for chromatic aberration correction and a convex lens. Also in 2x2 mode, we adopted a cemented lenslet array as shown in Fig.10.

Fig.11 shows the whole optical Layout of the NGS WFS. Focus adjustment of each of the four NGS WFS is performed by changing the distance between the pick-off mirror to the field stop. The entire optical system after the field stop moves with respect to the pick-off mirror. Fig.12 and Fig.13 show spot diagrams for each camera mode, and Tab.4 shows the spot size list for each mode. All spot sizes are less than 0.1 arcsec, which meets the specifications.

4.2 LGS WFS

The collimator is a single lens because the LGS has a single wavelength and does not require chromatic aberration correction. A Shack-Hartmann spot image is formed about 9 mm behind the MLA, but it isn't easy to place the detector here due to the short distance and space. Therefore, a relay lens is installed after the MLA to secure the space for the detector as well as to adjust the pixel scale. The relay lens consists of two lenses, one of which has a conical surface, which effectively corrects spherical aberration. Fig.14 shows the whole LGS WFS optical layout. As in the case of the NGS WFS, we move the entire optical elements after the field stop to adjust the focus to accommodate the change in the LGS height and the field location. Fig.15 shows a spot diagram and Tab.5 shows a spot size list. All spot size are less than 0.2 arcsec and meet the specifications.

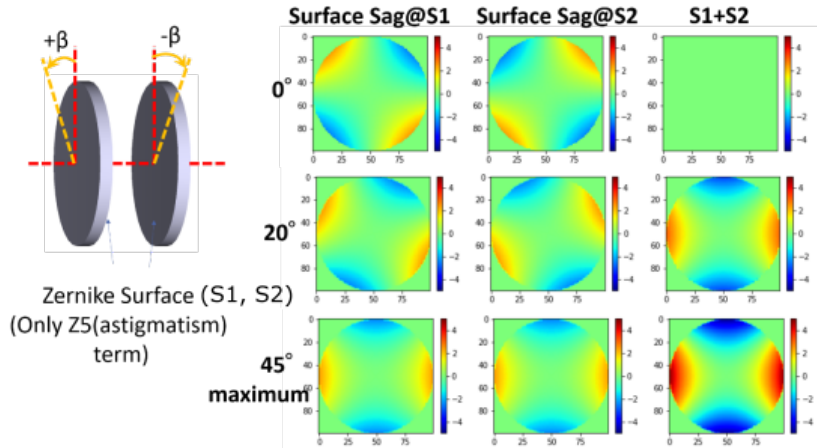


Figure 6. A schematic diagram of the astigmatism compensator

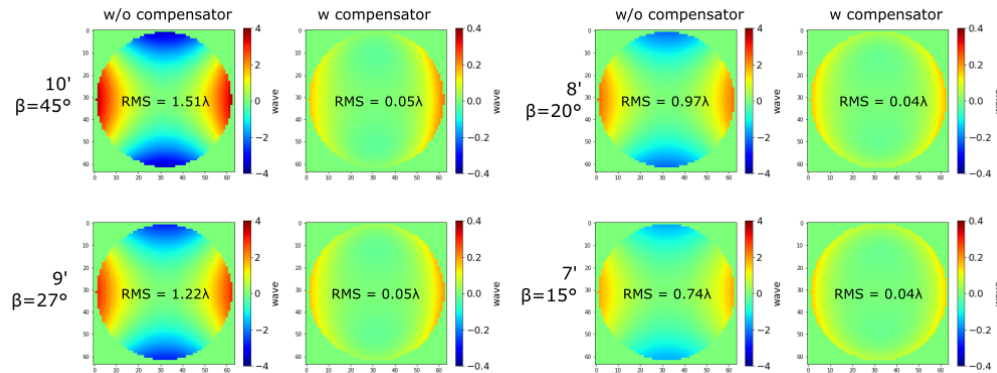


Figure 7. Wavefront aberration map before and after the astigmatism correction

In Fig.16 and Fig.17, the red and light blue lines represent the optical paths of the 80km LGS's 10 arcmin and 2 arcmin fields of view, respectively. The yellow and blue lines represent the optical paths in the 10 arcmin and 7 arcmin fields of view of NGS. All optical elements and opt-mechanics (which are not included in this figure) fit into the allocated space for WFS system.

5. TOLERANCE

5.1 NGS WFS

If the position of each optical element in the NGS WFS has uncertainties as given in Tab.6, the spot size can be changed as shown in Tab.7. In addition to the position errors, we considered the fabrication tolerances as shown in Tab.8, Tab.9, and Tab.10. We created 100 Monte-Carlo models, which included fabrication errors listed in these tables, and the maximum change in spot size is described in each table caption. Tab.11 shows the spot size changes by surface error of each mirror, such as pick-off mirror and fold mirrors. In the single-eye mode, the estimated spot size, which includes each element's position and fabrication errors, is calculated by RSS using the data in Tab.7, Tab.8, Tab.9, and Tab.11. The estimated spot size is $6.542\mu\text{m} = 0.075''$, which meets the specification. In the 2x2 mode, the estimated spot size is calculated using the data in Tab.7, Tab.8, Tab.10, and Tab.11. The estimated spot size is $7.133\mu\text{m} = 0.082''$, which meets the specification.

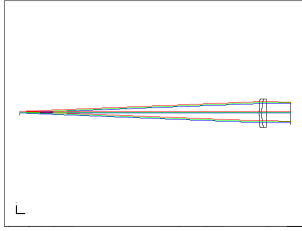


Figure 8. Collimator lens

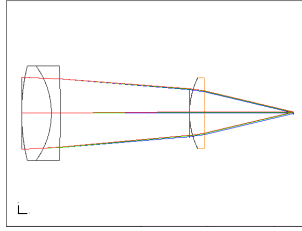


Figure 9. Camera lens

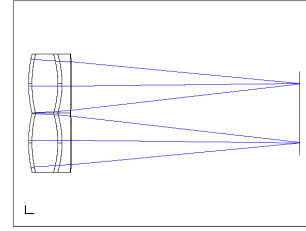


Figure 10. 2x2 Camera

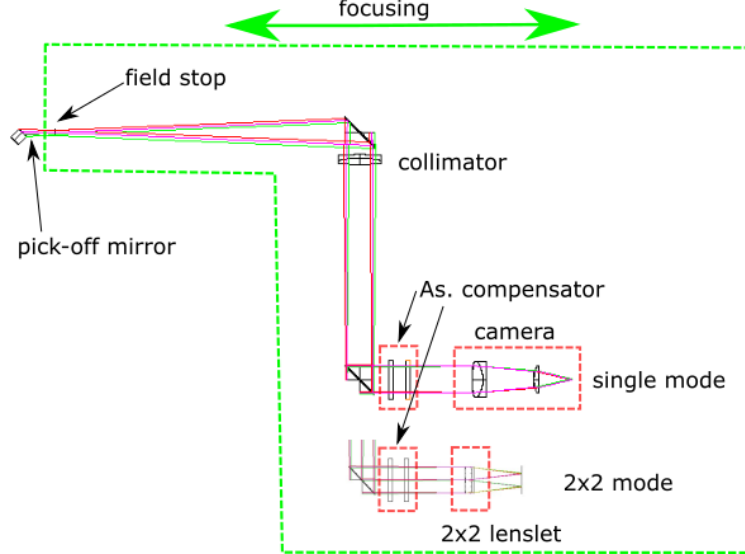


Figure 11. Layout of NGS WFS

5.2 LGS WFS

As in the case of the NGS WFS, if the position of each element in the LGS WFS has uncertainties as given in Tab.12, the spot size can be changed as shown in Tab.13. Also, we considered the fabrication tolerances shown in Tab.14 and Tab.15 for each optical element. We created 100 Monte-Carlo models, which included fabrication errors listed in these tables, and the maximum change in spot size is described in each table caption. Tab.16 shows the spot changes by surface error of each mirror. The estimated spot size, which includes each element's position and fabrication errors, is calculated by RSS using the data in Tab.13, Tab.14, Tab.15, and Tab.16. The estimated spot size is $2.593\mu\text{m} = 0.399''$, which meets the specification.

6. SUMMARY

We were able to design the WFS optical system for Ultimate-Subaru to meet the specifications within a given space. We also performed tolerance analysis to determine the position accuracy of each optical element required for opt-mechanical design. Also, since the lens manufacturing tolerances are achievable values, we do not see any issues in manufacturing the optics for the GLAO WFS system that meets the specifications.

REFERENCES

- [1] Foley, J. P. and Campbell, C., "An optical device with variable astigmatic power," *Optometry and Vision Science* **76**, 664-667 (1999).

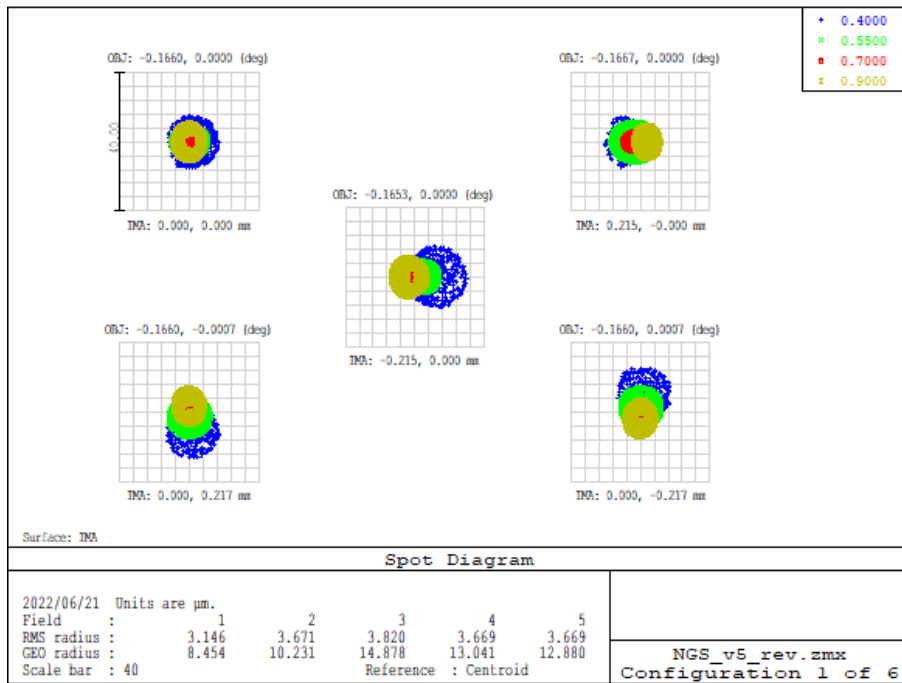


Figure 12. Spot diagram of single-eye mode

Table 4. Spot Size

	single-eye mode		2x2 mode	
	[μm]	[arcsec]	[μm]	[arcsec]
Field 1	3.146	0.04	5.509	0.06
Field 2	3.671	0.04	5.510	0.06
Field 3	3.820	0.04	5.799	0.07
Field 4	3.669	0.04	5.443	0.06
Field 5	3.669	0.04	5.962	0.07

Table 5. Spot Size

	[μm]	[arcsec]
Field 1	0.466	0.07
Field 2	0.481	0.07
Field 3	0.489	0.08
Field 4	0.856	0.13
Field 5	3.669	0.16

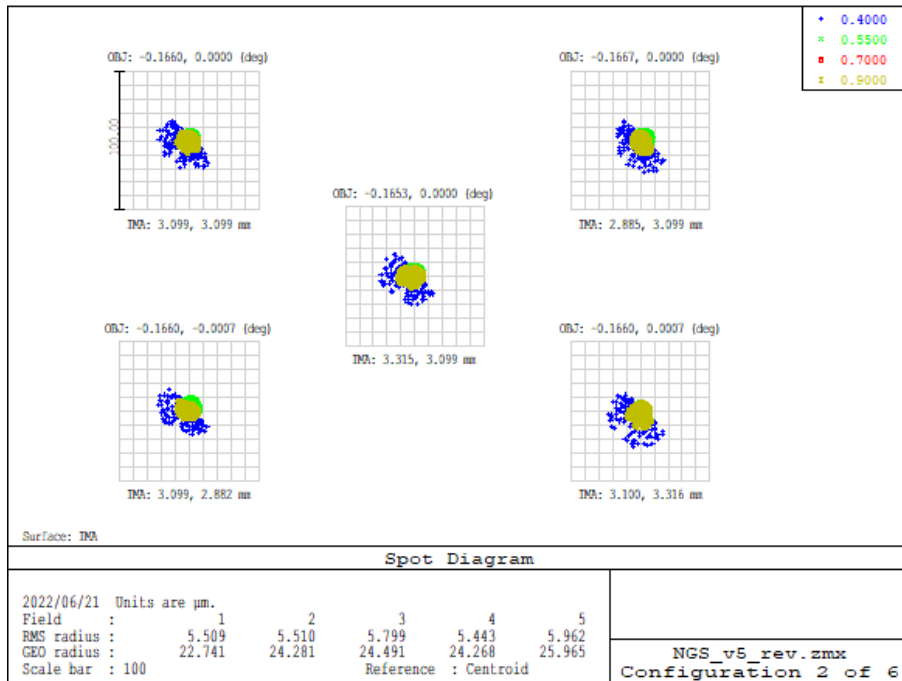


Figure 13. Spot diagram of 2x2 mode

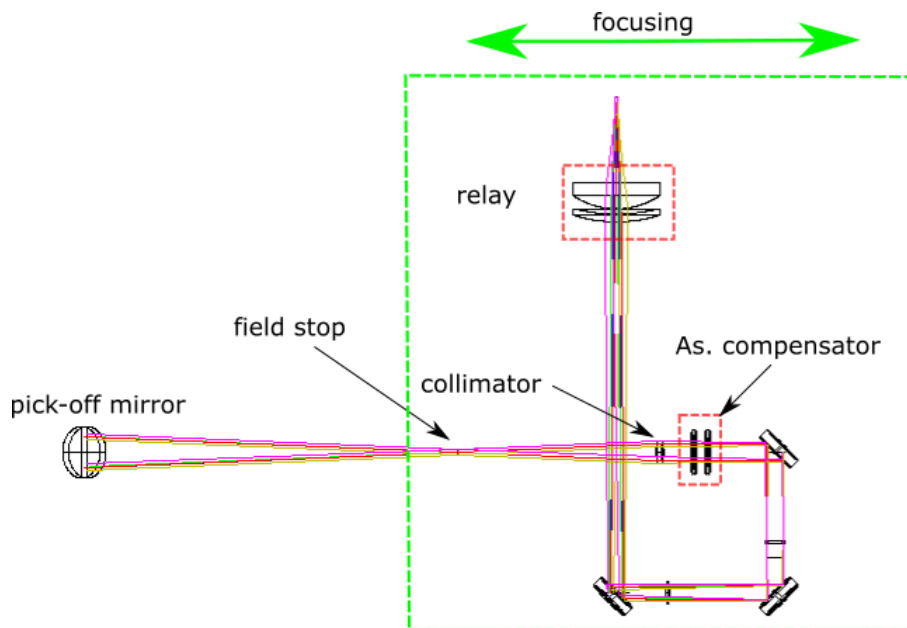


Figure 14. Layout of LGS WFS

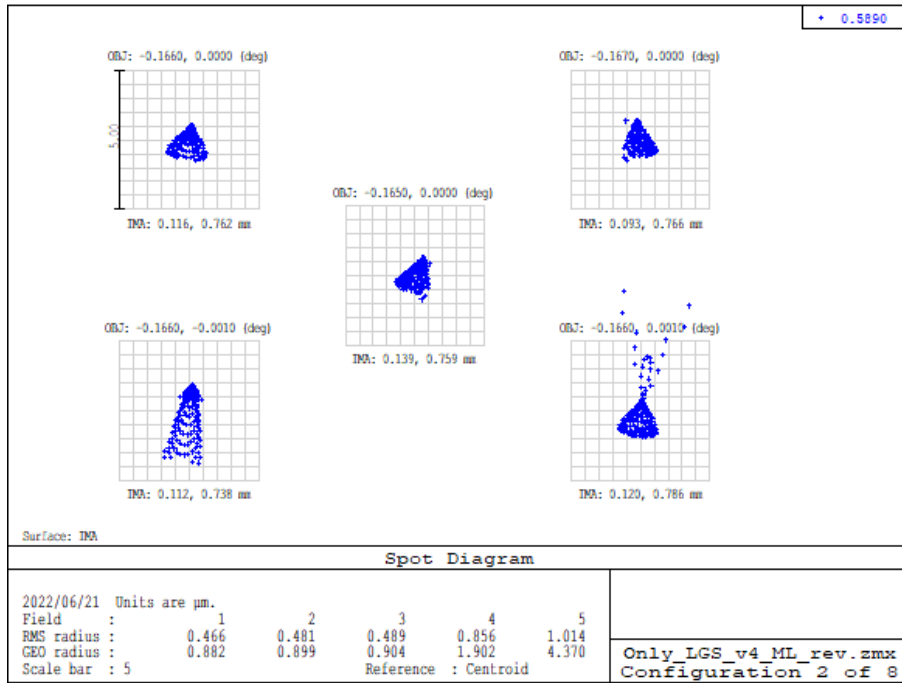


Figure 15. Spot Diagram

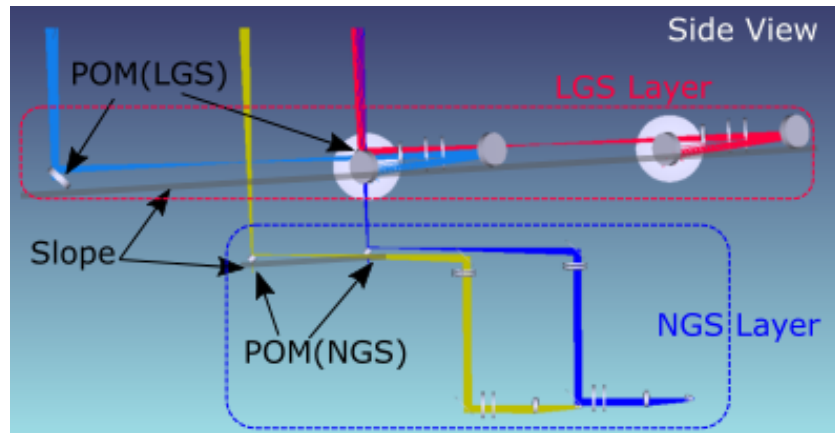


Figure 16. Side View of the layout of NGS and LGS

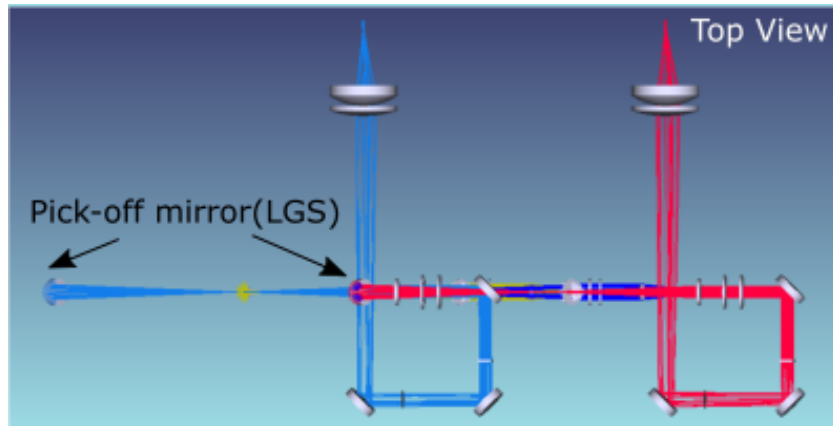


Figure 17. Top View of the layout of NGS and LGS

Table 6. Position Error List (NGS)

	Shift [mm]			Tilt [degree]	
	Z	X	Y	X	Y
PickOff	0.1	—	—	0.05	0.05
FM1	0.1	—	—	0.1	0.1
Collimator	0.1	0.1	0.1	0.1	0.1
Astigmatism Compensator	0.2	0.2	0.2	0.2	0.2
FM2	0.1	—	—	0.1	0.1
Camera 1	0.1	0.05	0.05	0.1	0.1
Camera 2	0.1	0.1	0.1	0.1	0.1
Camera barrel	0.1	0.1	0.1	0.1	0.1
2x2 Lens array	0.05 ^a	0.1	0.1	0.1	0.1
Detector	—	—	—	0.004	0.004

^a focal length variation among the four lenslet

Table 7. Spot Size change[um] (NGS WFS)

	Shift [mm]			Tilt [degree]	
	Z	X	Y	X	Y
PickOff	0.213	—	—	0.141	0.213
FM1	0.335	—	—	0.284	0.284
Collimator	0.131	0.027	0.027	0.014	0.014
Astigmatism Compensator	0.000	0.001	0.001	0.003	0.003
FM2	0.001	—	—	0.423	0.423
Camera 1	0.293	0.378	0.378	0.014	0.014
Camera 2	0.100	0.740	0.740	0.102	0.102
Camera barrel	0.0011	0.069	0.069	0.241	0.241
2x2 Lens array	2.535 ^a	0.034	0.034	0.023	0.023
Detector	—	—	—	0.004	0.004
RSS (single-eye mode)	1.545 [um]				
RSS (2x2 mode)	2.681 [um]				

^a caused by focal length variation among the four lenslet

Table 8. Fabrication Tolerances of Collimator (NGS)

		curvature error	irregularity	thickness	index
G1	R1	±5 fringes	1 fringe	±0.1mm	0.001
	R2	±5 fringes	1 fringe		
G2	R1	±5 fringes	1 fringe	±0.1mm	0.001
	R2	±5 fringes	1 fringe		

decenter is less than 1' after cemented G1 and G2

The worst spot change = 1.328[um] among 100 Monte-Carlo data

Table 9. Fabrication Tolerances of Camera (NGS)

		curvature error	irregularity	thickness	decenter	index
G1	R1	±3 fringes	0.2 fringe	±0.1mm	less than <30" after cemented	0.001
	R2	±3 fringes	0.2 fringe			
G2	R1	±3 fringes	0.2 fringe	±0.1mm		
	R2	±3 fringes	0.2 fringe			
G1	R1	±3 fringes	0.2 fringe	±0.1mm	<1'	0.001
	R2	±3 fringes	0.2 fringe			

The worst spot change = 1.692[um] among 100 Monte-Carlo data

Table 10. Fabrication Tolerances of 2x2 lens array (NGS)

		curvature error	irregularity	thickness	decenter	index
G1	R1	±5 fringes	1 fringe	±0.1mm	1'	0.001
	R2	±5 fringes	1 fringe			
G2	R1	±5 fringes	1 fringe	±0.1mm	1'	0.001
	R2	±5 fringes	1 fringe			

decenter is less than 1' after cemented G1 and G2
 The worst spot change = 1.219[um] among 100 Monte-Carlo data

Table 11. Surface accuracy of mirrors (NGS)

	surface accuracy	Spot change[um]
pick-off mirror	1/10λ	0.048[um]
Fold mirror1	1/10λ	0.522[um]
Fold mirror2	1/10λ	0.260[um]

Table 12. Position Error List (LGS)

	Shift [mm]			Tilt [degree]	
	Z	X	Y	X	Y
PickOff	0.2	—	—	0.05	0.05
Collimator	0.2	0.1	0.1	0.2	0.2
Astigmatism Compensator	0.2	0.2	0.2	0.2	0.2
FM1	0.1	—	—	0.05	0.05
MLA	0.1	—	—	0.2	0.2
FM2	0.1	—	—	0.05	0.05
FM3	0.1	—	—	0.05	0.05
relay 1	0.1	0.1	0.1	0.05	0.05
relay 2	0.1	0.1	0.1	0.1	0.1
relay barrel	0.2	0.2	0.2	0.1	0.1
Detector	—	—	—	0.1	0.1

Table 13. Spot Size Changes[um] (LGS WFS)

	Shift			Tilt	
	Z	X	Y	X	Y
PickOff	0.014	—	—	0.413	0.046
Collimator	0.028	0.017	0.249	0.031	0.002
Astigmatism Compensator	0.026	0.004	0.004	0.003	0.001
FM1	0.1	—	—	0.485	0.034
MLA	0.21	—	—	0.072	0.002
FM2	0.347	—	—	0.367	0.024
FM3	0.352	—	—	0.233	0.014
relay 1	0.202	0.124	0.211	0.199	0.121
relay 2	0.037	0.125	0.139	0.087	0.046
relay barrel	0.420	0.021	0.137	0.219	0.045
Detector	—	—	—	0.078	0.012
RSS	1.192 [um]				

Table 14. Fabrication Tolerances of Collimator (LGS)

		curvature error	irregularity	thickness	decenter	index
G1	R1	±5 fringes	1 fringe	±0.1mm	<1'	0.001
	R2	±5 fringes	1 fringe			

The worst spot change = 0.229[um] among 100 Monte-Carlo data

Table 15. Fabrication Tolerances of relay lens (LGS)

		curvature error	irregularity	thickness	decenter	index
G1	R1	±5 fringes	1 fringe	±0.1mm	1'	0.001
	R2	±5 fringes	1 fringe			
G2	R1	±5 fringes	1 fringe	±0.1mm	2'	0.001
	R2	±5 fringes	1 fringe			
R1 conic constant error ±0.002						

The worst spot change = 0.899[um] among 100 Monte-Carlo data

Table 16. Surface accuracy of mirrors (LGS)

	surface accuracy	Spot change[um]
pick-off mirror	1/10λ	0.009[um]
Fold mirror1	1/10λ	0.010[um]
Fold mirror2	1/10λ	0.001[um]
Fold mirror3	1/10λ	0.500[um]